AIAA SciTech Forum
January 3-7, 2022, San Diego, CA & Virtual
AIAA SCITECH 2022 Forum

10.2514/6.2022-0885

A Technique for Matching Propeller, Motor, and Airframe of an Electric Powered Aircraft Based on Efficiency Maps

Hak-Tae Lee*
Inha University, Incheon, Republic of Korea, 21999

Electric propulsion has been widely used for small unmanned aircraft for more than two decades. Even though the electric motors are known to be fairly efficient, ensuring that the high efficiency operating regions of all the key components, motor, propeller, and airframe is not straight forward. This paper proposes a performance map based methodology for analyzing the efficiencies of motors, fixed pitch propellers, and airframe together at a wide range of operating conditions. Using this methodology, designers can have a full view of the component efficiencies as well as the combined efficiency at design and off design points. It will also be useful for checking the propulsion component selection and will provide guidelines for finding better matching components to increase the overall system efficiency.

Nomenclature

$\mathcal{A}$	=	wing aspect ratio
C_D	=	aircraft drag coefficient
C_{Dp}	=	parasite drag coefficient
C_L	=	aircraft lift coefficient
C_P	=	propeller power coefficient
C_T	=	propeller thrust coefficient
D	=	propeller diameter, m
$\mathcal{D}$	=	aircraft drag, N
e	=	span efficiency
$\dot{h}$	=	climb rate, m/s
i_a	=	armature current, A
J	=	advance ratio
K_t	=	motor torque constant, Nm/A
K_e	=	motor back emf constant, Vs
k	=	induced drag parameter
n	=	rotational speed, rev/s
P	=	power, W
Q	=	torque, Nm
Q_f	=	friction torque, Nm
r	=	resistance, Ω
rpm	=	rotational speed, rev/min
S	=	wing area, m^2
$\mathcal{T}$	=	thrust, N
V	=	flight speed, m/s
v	=	voltage, V
W	=	aircraft weight, N
η_p	=	propeller efficiency
η_m	=	motor efficiency
η	=	combined motor and propeller efficiency
ρ	=	air density, kg/m^3
ω	=	rotational speed, rad/s

*Associate Professor, Department of Aerospace Engineering, 36 Gaetbeol-Ro, Yeonsu-Gu, Incheon, AIAA Senior Member.

I. Introduction

EVEN though the analyses and measurements have been extensively performed for major electric propulsion components including propeller, motor, electronic speed control, and airframe, an intuitive and straightforward way of evaluating overall system efficiency as well as the impacts of off design flight conditions have not been presented.

McDonald [1, 2] partially addressed this problem using a motor efficiency map with respect to rotational speed and torque, which was the foundation of this study. However, the subsequent work [3] focused on variable pitch propellers, which are more advantageous for matching the efficiencies. D'Sa *et al.* [4] attempted to visualize the efficiencies of a given propeller by varying the size of the data points in the thrust coefficient curve plotted with respect to advance ratio. Park *et al.* [5] presented a methodology to find the best motor and propeller combination among the given candidates for a hybrid drone using an internal combustion engine, generator, and electric motors. An engine efficiency map that shows the contours of specific fuel consumption as functions of rotational speed and torque similar to the motor efficiency map of McDonald [1, 2] was used. Duan *et al.* [6] approached this problem using a particle swarm optimization algorithm to find the optimum propeller geometry with given motor and flight conditions. In this work, propeller torque curve was overlaid on top of the motor efficiency map, but numerical iterations were used for the optimization. Bartlett [7] also tried to numerically find the rpm that makes the motor output power and the propeller input power the same.

Some of the other work focused on the Electric Speed Control (ESC). Gong and Verstraete [8] investigated the efficiencies of several commercial off the shelf ESCs. Their measurements showed that the ESCs are generally more efficient at higher power outputs. ESC is not included in the current study, but it can also be incorporated within the same framework.

This paper approaches the motor-propeller-airframe matching problem by drawing contours of key parameters including motor efficiency, propeller efficiency, flight speed, and climb rate. As in [1], rotational speed and torque output of the motor are identified as the key independent variables. It is shown that, with given motor, propeller, and airframe, motor efficiency, propeller efficiency, forward flight speed, and climb rate are uniquely determined as functions of rpm and torque. Once all the contours are plotted together, it is possible to determine the overall system efficiency at a wide range of operating conditions. If there exists a mismatch of efficiencies between components, designers can identify the source and find solutions using those contours.

Following this Introduction, Section II presents how motor efficiency, propeller efficiency, and climb rates are calculated and plotted. Section III shows the combined contours using an example. Section IV concludes this paper.

II. Electric Propulsion Components

General flow of power in an electric propulsion system is described in Fig. 1. For the current study, ESC efficiency is not considered. Propeller is the key component that is connected to the motor through rotational parameters, rpm and torque, and connected to the airframe through linear motion parameters, thrust and flight speed. In this study, rpm and torque are chosen as the two independent variables. In the following subsections, it is demonstrated that all efficiencies and climb rates are uniquely determined by rpm and torque, and their contours provide clear view of the propulsion system matching status.

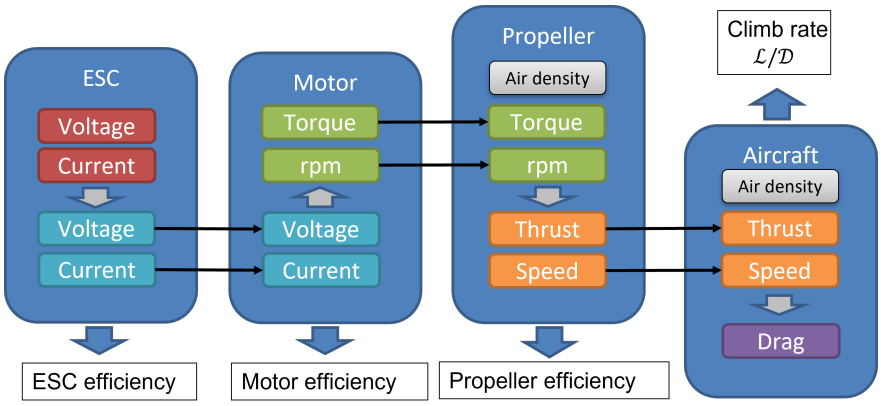

Fig. 1 Energy flow of an electric propulsion system.

A. Motor

For this paper, a simple DC motor model is used; however, the same procedure can be applied to more sophisticated motor models or measurement data. Since the electromagnetic torque, which is a sum of motor output torque, Q, and friction torque, Q_f, is proportional to the current flowing in the motor armature, i_a, the current can be expressed as in Eq. (1) where K_t denotes the motor's torque constant.

$$i_a = \frac{Q + Q_f}{K_t} \tag{1}$$

The back electromagnetic force (EMF) voltage, v_{emf}, is proportional to the rotational speed, ω, as shown in Eq. (2) where K_e is the back EMF constant.

$$v_{emf} = K_e \omega \tag{2}$$

The voltage applied to the motor, v, is the sum of the voltage drop from the armature resistance, r, and the back EMF voltage as shown in Eq. (3).

$$v = i_a r + v_{emf} = i_a r + K_e \omega \tag{3}$$

Motor efficiency, η_m, is the output mechanical power divided by the input electric power as shown in (4).

$$\eta_m = \frac{Q\omega}{v i_a} \tag{4}$$

This process is summarized in Fig. 2. Friction torque, Q_f, is generally a function of the rotational speed, which reflects the frictions from the bearing and the aerodynamic resistant torque of the rotor. As stated previously, the proposed method can be applied to more sophisticated motor models or measurement data as far as the motor efficiency is uniquely determined as a function of rpm and torque.

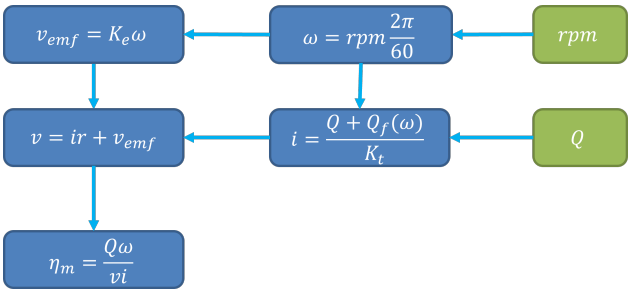

Fig. 2 Calculation of motor efficiency from rpm and torque.

Figure 3 shows example motor efficiency and voltage contours assuming a constant friction torque. Sample operating point 1 represents a condition where the applied voltage is 8 V. If the load torque is 0.26 Nm, the motor will spin at 7500 RPM, and the efficiency is 85 %. In sample operating point 2, applied voltage is 4.5 V. For the load torque is 0.12 Nm, the motor will spin at 4000 RPM at an efficiency of 82 %.

B. Propeller

Advance ratio, J, is defined in Eq. (5). In reality, the propeller thrust and power coefficients, C_T and C_P, are functions of rpm in addition J due to the Reynolds number effects. Since rpm is one of the two independent variables, these effects can be incorporated if desired. For the current study, it is assumed that C_T and C_P are functions of J only as shown in Eqs. (6) and (7) for simplicity.

$$J = \frac{V}{nD} \tag{5}$$

$$C_T = C_T(J) \tag{6}$$

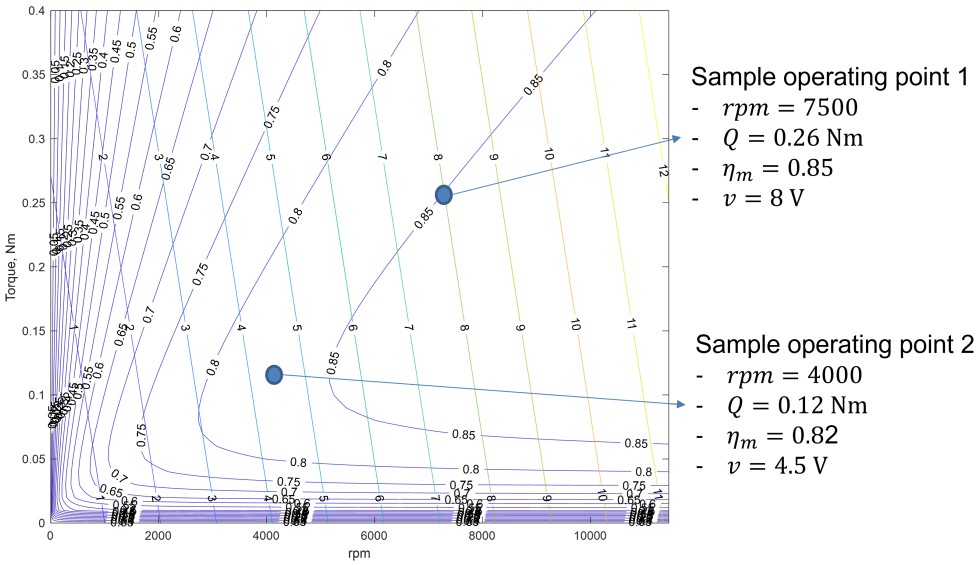

Fig. 3 Motor efficiency and torque contours.

$$C_P = C_P(J) \tag{7}$$

From a given pair of rpm and torque, the shaft power is calculated as in Eq. (8).

$$P = Q\omega \tag{8}$$

Propeller power coefficient is calculated using the definition of C_P in Eq. (9).

$$C_P = \frac{P}{\rho n^3 D^5} \tag{9}$$

J that corresponds to the C_P from Eq. (9) needs to be found using propeller data that are obtained through measurements or propeller analysis tools. One possible issue is that, for some propellers, for smaller Js where the C_P stays relatively constant, the corresponding J may not be unique. For this study, it is assumed that J can be uniquely determined. This assumption is reasonable in the sense that the propeller efficiency is small in the region where the C_P curve is relatively flat. Once the J is found, corresponding C_T can be found. Forward speed, V, propeller efficiency, η_p, and thrust, $\mathcal{T}$, can be calculated using Eqs. (10) through (12), respectively.

$$V = JnD \tag{10}$$

$$\eta_p = J\frac{C_T}{C_P} \tag{11}$$

$$\mathcal{T} = C_T(J)\,\rho n^2 D^4 \tag{12}$$

The propeller analysis process is summarized in Fig. 4. Note that the forward flight speed is uniquely determined by Eq. (10) from rpm and torque, which becomes the key connection between the propeller and airframe. rpm, ω, and n shown in Fig. 4 are the same rotational speeds with different units. In this study, all three units are used so that common conventions or data representations in each component can be readily utilized.

An example propeller performance map is shown in Fig. 5. Colored regions represent the propeller efficiency. It can be observed that, for this particular propeller that has a maximum efficiency of about 73 %, high efficiency region is narrow, especially compared to the high efficiency regions of the motor in Fig 3. Solid black lines denote the forward speed contours, and the solid blue lines represent the thrust contours.

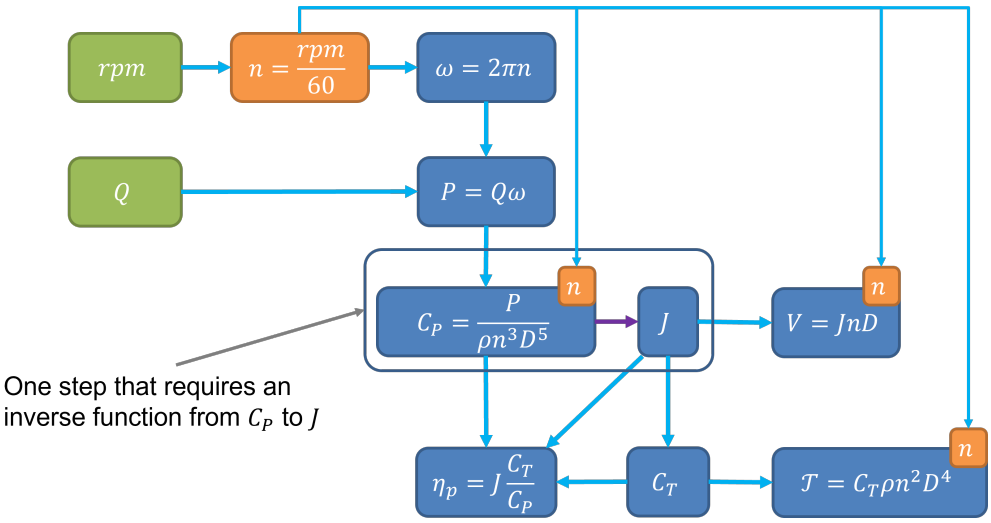

Fig. 4 Calculation of propeller efficiency, thrust, and speed from rpm and torque.

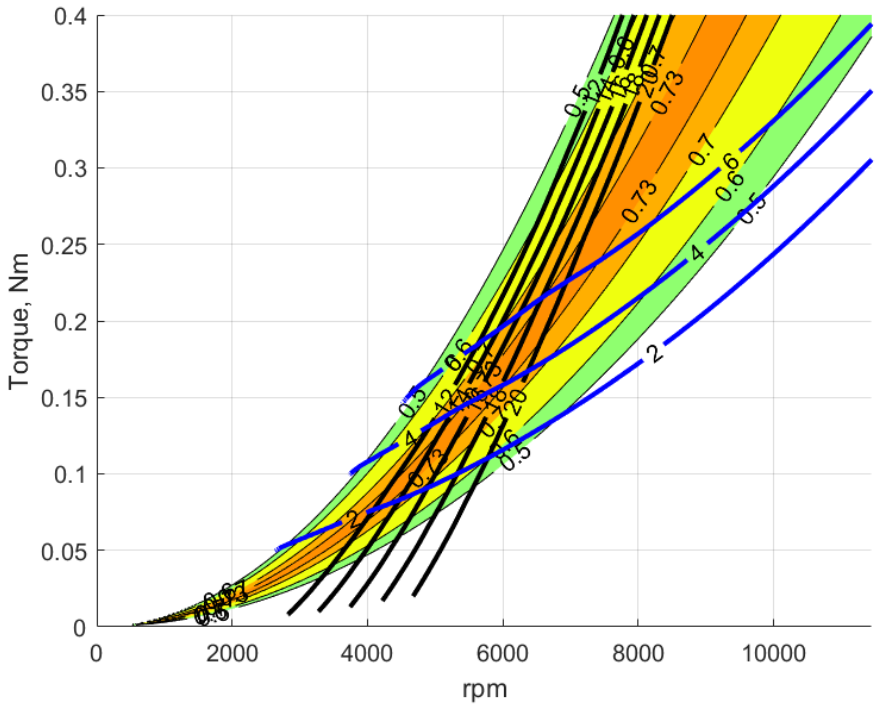

Fig. 5 Propeller efficiency, thrust, and forward speed contours.

C. Airframe

The simplest model of aircraft includes the reference wing area, S, weight, W, parasite drag coefficient, C_{D_P}, and induced drag parameter, k, where k is defined by Eq. (13). Drag coefficient, C_D, is a function of lift coefficient, C_L, as described in (14).

$$k = \frac{1}{\pi e \mathcal{A}} \tag{13}$$

$$C_D = C_{D_P} + k{C_L}^2 \tag{14}$$

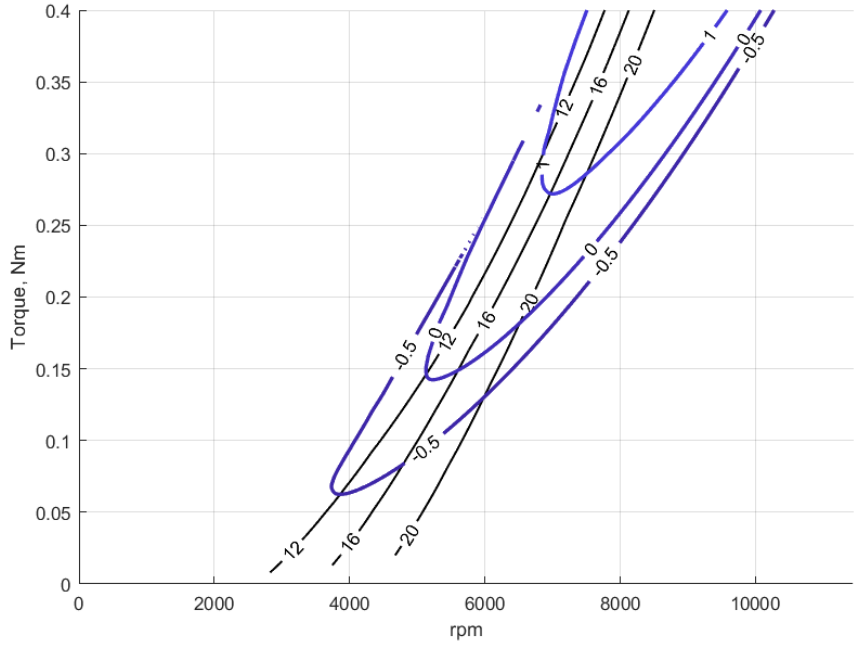

Fig. 6 Example $\dot{h}$ contours for three climb rate values, -0.5, 0, and 1.0 m/s.

Drag, $\mathcal{D}$, of an aircraft is a function of V as described in Eq. (15). The drag has to be equal to the $\mathcal{T}$ of the propeller from Eq. (12) when the aircraft is at a steady level flight. However, finding the rotational speed that satisfies the equality is not straightforward because $\mathcal{T}$, which is a function of C_T, is again a function of n as shown in Eq. (12).

$$\mathcal{D} = \frac{1}{2}\rho S C_{D_p} V^2 + \frac{kW}{\frac{1}{2}\rho S}\frac{1}{V^2} \tag{15}$$

This issue can be avoided by calculating the climb rate, $\dot{h}$, using Eq. (16) instead of matching the drag and thrust. The contour for $\dot{h} = 0$ is the one that represents level flight. Contours of non-zero climb rates show the operational points for different climb and descent conditions. Figure 6 shows example contours for three different conditions. Note that these climb rate contours requires propeller performance data. In Fig. 6, solid black lines denote contours of three different flight speeds, 12, 16, and 20 m/s, respectively. Solid blue lines show the climb rate contours for -0.5, 0, and 1.0 m/s, respectively. Figure 7 summarizes the process of computing the climb rate using the thrust and speed from the propeller analysis.

$$\dot{h} = \frac{\mathcal{T} - \mathcal{D}}{W} V \tag{16}$$

III. Example Analysis

Using the techniques described in Section II, an example case is presented. Table 1 summarizes the parameters of an AXI 4120/20 brushless motor used for this example. For this study, K_e is assumed to be identical to K_t. Figure 8 shows the C_T and C_P curves as functions of J for an APC Slow Flyer 11 by 7 propeller [9]. Table 2 summarizes the airframe parameters. The drag polar represents an aircraft with a relatively small drag without any fixed landing gear or other protrusions such as antennas or cameras. 1.2 kg/m^3 is used for the air density assuming low altitude operations.

Figure 9 shows contours of motor efficiency, propeller efficiency, and climb rates along with flight speed, voltage, and thrust. The figure is cluttered and not easy to read. Figure 10 shows the region along the climb rate contour that represents level flight. Three operational points are marked for speeds of 12, 16 and 20 m/s and all the performance parameters are listed in Table 3. One of the ways to interpret these results is to consider control inputs and corresponding

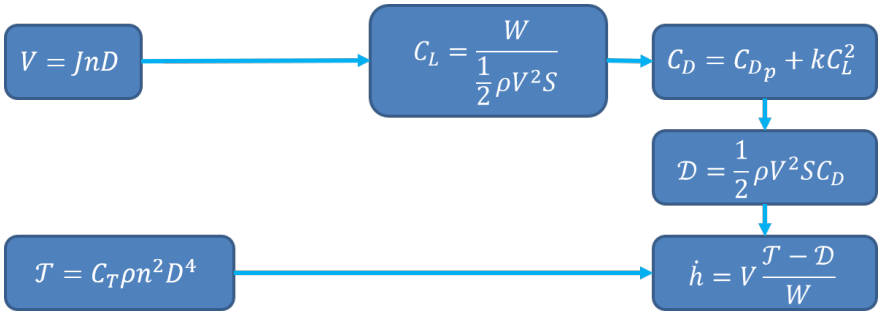

Fig. 7 Calculation of climb rate from flight speed and thrust.

Table 1 Motor parameters for an AXI 4120/20 BLDC motor.

Parameter	Value
K_t	0.0103 Nm/A
r	0.027 Ω
Q_f	0.0144 Nm

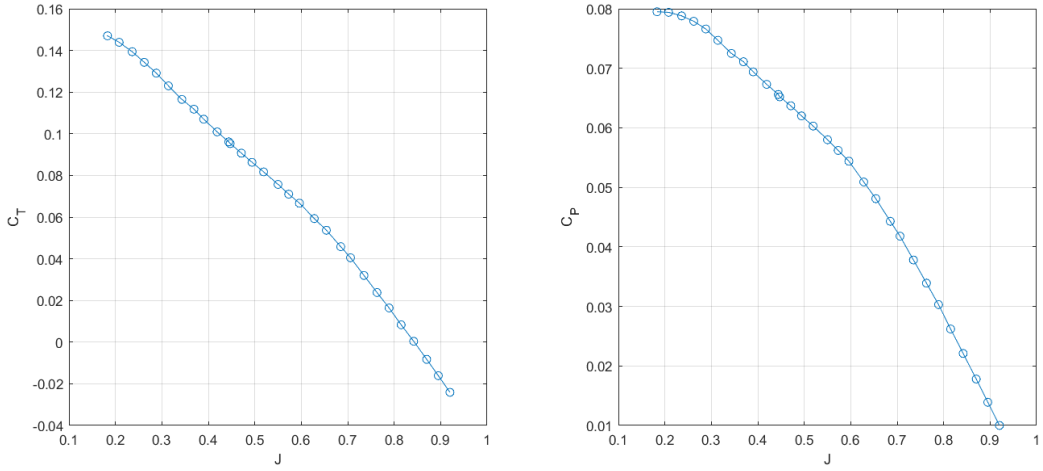

Fig. 8 C_T and C_P data of an APC 11 x 7 propeller. [9]

Table 2 Airframe parameters.

Parameter	Value
Wing area, S	0.7254 m^2
Mass, m	7.4 kg
C_{D_p}	0.019
k	0.04

outputs. If a voltage of 6.5 V is applied to the motor and the aircraft's elevator angle is adjusted so that the aircraft maintains level flight, it will fly at 16 m/s while the propeller is spinning at 5600 rpm.

Once the selection of components are finalized, motor and propeller efficiency can be multiplied to form the total propulsion efficiency, η, as shown in Fig. 11. It shows that for speeds larger than the minimum power speed, level flight conditions are well within the high efficiency region. It also suggests that slightly larger speed is advantageous for

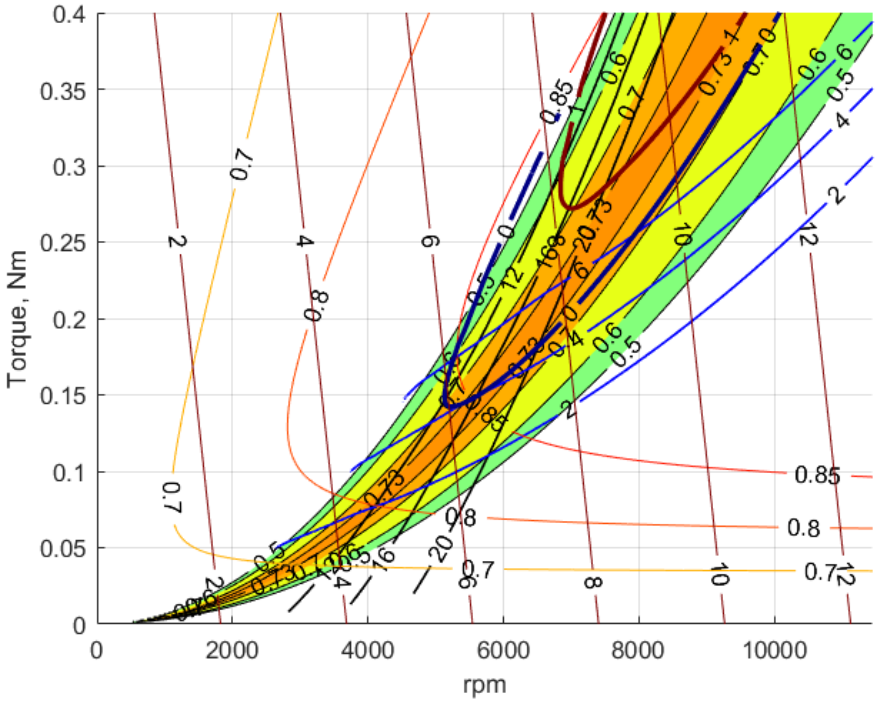

Fig. 9 Complete performance map.

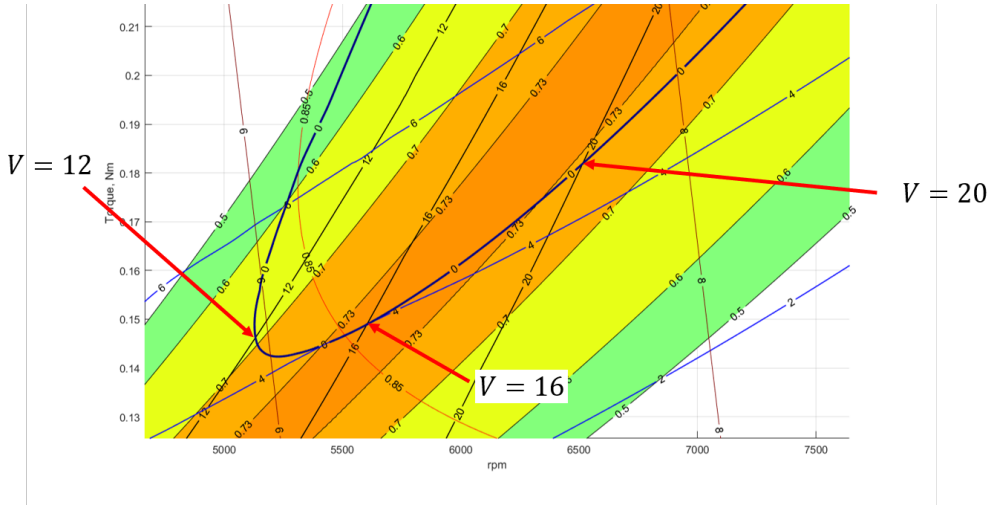

Fig. 10 Magnified view of the complete set of contours around the level flight condition.

Table 3 Complete performance parameters for three level flight speeds, 12, 16, and 20 m/s.

V (m/s)	C_L	L/D	$\mathcal{T}$ (N)	v (V)	rpm	Q (Nm)	η_m (%)	η_p (%)	η (%)
12	1.16	16.0	4.54	5.9	5130	0.146	84.6	69.3	58.6
16	0.65	18.1	4.00	6.5	5600	0.149	85.1	73.2	62.3
20	0.42	16.0	4.51	7.5	6510	0.182	86.3	72.7	62.3

moderate climb rates in terms of propulsion efficiency.

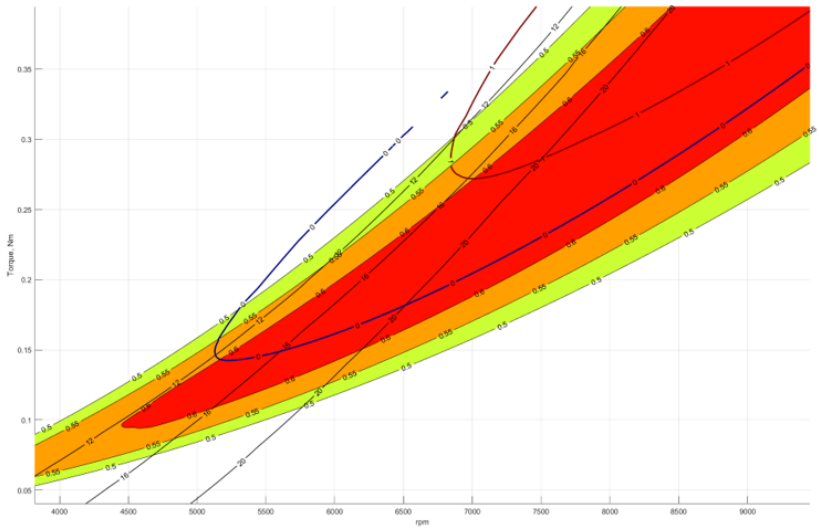

Fig. 11 Combined efficiency map.

IV. Conclusions

A methodology that shows the complete view of the efficiencies and performance parameters of an electric propulsion system is presented. By plotting contours of motor efficiency, propeller efficiency, and climb rate, it is possible to check whether the high efficiency region of each component is aligned with another and to identify what is required to improve the overall efficiency. This method also provides a comprehensive means of finding efficiencies and performance parameters at a wide range of operating conditions.

Acknowledgments

This work was sponsored by Inha University.

References

[1] McDonald, R. A., "Optimal Propeller Pitch Scheduling and Propeller–Airframe Matching for Conceptual Design," *15th AIAA Aviation Technology, Integration, and Operations Conference*, 2015. https://doi.org/10.2514/6.2015-3190, URL https://arc.aiaa.org/doi/abs/10.2514/6.2015-3190.

[2] McDonald, R. A., "Modeling of Electric Motor Driven Propellers for Conceptual Aircraft Design," *53rd AIAA Aerospace Sciences Meeting*, 2015. https://doi.org/10.2514/6.2015-1676, URL https://arc.aiaa.org/doi/abs/10.2514/6.2015-1676.

[3] McDonald, R. A., "Modeling of Electric Motor Driven Variable Pitch Propellers for Conceptual Aircraft Design," *54th AIAA Aerospace Sciences Meeting*, 2016. https://doi.org/10.2514/6.2016-1025, URL https://arc.aiaa.org/doi/abs/10.2514/6.2016-1025.

[4] D'Sa, R., Jenson, D., Henderson, T., Kilian, J., Schulz, B., Calvert, M., Heller, T., and Papanikolopoulos, N., "SUAV:Q - An improved design for a transformable solar-powered UAV," *2016 IEEE/RSJ International Conference on Intelligent Robots and Systems (IROS)*, 2016, pp. 1609–1615. https://doi.org/10.1109/IROS.2016.7759260.

[5] Park, J.-H., Lyu, H.-G., and Lee, H.-T., "Power System Optimization for Electric Hybrid Unmanned Drone," *Journal of the Korean Society for Aeronautical Space Sciences*, Vol. 47, No. 4, 2019, pp. 300–308. https://doi.org/10.5139/JKSAS.2019.47.4.300.

[6] Duan, D., Wang, Z., Wang, Q., and Li, J., "Research on Integrated Optimization Design Method of High-Efficiency Motor Propeller System for UAVs With Multi-States," *IEEE Access*, Vol. 8, 2020, pp. 165432–165443. https://doi.org/10.1109/ACCESS.2020.3014411.

[7] Bartlett, B., "Simulation of a Configurable Hybrid Aircraft," Master's thesis, Cal Poly, 2021.

[8] Gong, A., and Verstraete, D., "Experimental Testing of Electronic Speed Controllers for UAVs," *53rd AIAA/SAE/ASEE Joint Propulsion Conference*, 2017. https://doi.org/10.2514/6.2017-4955, URL https://arc.aiaa.org/doi/abs/10.2514/6.2017-4955.

[9] Brandt, J. B., Deters, R. W., Ananda, G. K., Dantsker, O. D., and Selig, M. S., "UIUC Propeller Database," , 2020. URL https://m-selig.ae.illinois.edu/props/propDB.html.